Multiple bound states in scissor-shaped waveguides

Evgeny N. Bulgakov,[1] Pavel Exner,[2,3,*] Konstantin N. Pichugin,[1] and Almas F. Sadreev[1,4,†]
[1]*Institute of Physics, 660036 Krasnoyarsk, Russia*
[2]*Nuclear Physics Institute, Czech Academy of Sciences, 25068 Řež, Czechia*
[3]*Doppler Institute, Czech Technical University, Břehová 7, 11519 Prague, Czechia*
[4]*Department of Physics and Measurement Technology, Linköping University, 581 83 Linköping, Sweden*
(Received 20 June 2002; revised manuscript received 29 July 2002; published 23 October 2002)

We study bound states of the two-dimensional Helmholtz equations with Dirichlet boundary conditions in an open geometry given by two straight leads of the same width which cross at an angle θ. Such a four-terminal junction with a tunable θ can realized experimentally if a right-angle structure is filled by a ferrite. It is known that for $\theta=90°$ there is one proper bound state and one eigenvalue embedded in the continuum. We show that the number of eigenvalues becomes larger with increasing asymmetry and the bound-state energies are increasing as functions of θ in the interval $(0,90°)$. Moreover, states which are sufficiently strongly bound exist in pairs with a small energy difference and opposite parities. Finally, we discuss how the bound states transform with increasing θ into quasibound states with a complex wave vector.

DOI: 10.1103/PhysRevB.66.155109 PACS number(s): 42.25.Bs, 03.65.Ge, 73.40.Lq, 03.75.Be

I. INTRODUCTION

The question of the possible existence of modes trapped in open two-dimensional systems has been a classic in the theory of waveguides; trapped modes due to particular boundary conditions were studied already half a century ago.[1] However, only much later was it realized that the introduction of bends and crossing into waveguides gives rise generally to confined states, or bound states, which exist below the cutoff frequency for the waveguide.[2–16] The existence of such states has both theoretical significance and implications for possible applications. They have been subsequently discussed in many papers; in addition to those mentioned above we refer the reader to Ref. 17 and the bibliography therein.

In this paper we consider a system of two straight waveguides of the same width d which cross at a nonzero angle θ. The right-angle case was one of the first examples where the binding was studied. Schult, Ravenhall, and Wyld[7] showed the existence of two bound states. One of them is a true bound state at energy $0.66(\pi/d)^2$ in natural units, while the other one at $3.72(\pi/d)^2$ is embedded into the continuum and does not decay due to the symmetry. The latter corresponds to the single bound state in an L-shaped tube of width $d/2$.[5] Our aim is to show how the spectrum of such a junction, which we will call for the sake of brevity ''scissors'' in the following, changes as the angle θ varies over the interval $(0,90°)$.

We will show that as we go further from the cross symmetry of the right-angle structure, new bound states emerge from the continuum. In strongly skewed junctions corresponding to a small θ there are many of them. The mechanism responsible for their existence is the same as for the bound states in sharply broken tubes studied theoretically and experimentally in Refs. 10 and 12, namely, a long part of the junction where there transverse contribution to the energy is substantially lower than $(\pi/d)^2$. In the present case, however, the system has a mirror symmetry with respect to the axis of the complement angle $180°$-θ and the bound states exist in pairs corresponding to different parity. We will show that as the angle θ diminishes and the states become strongly bound, the energy gap between the even and odd members of the pair vanishes exponentially fast. We also study the behavior around the critical values θ_c where the bound states emerge from the continuum. Our numerical analysis shows that the binding energy of the weakly coupled states behaves as $\approx\pi^2-\gamma(\theta_c-\theta)^2$ for θ slightly below θ_c; above this value we have instead a quasibound state.

II. BOUND STATES AND RESONANCES

First we review some properties of the bound states in scissor systems which follow from general principles such as their symmetries and dependence on the geometry. The methods one can employ to this aim are rather standard and explained in detail in classical textbooks,[18,19] so we describe them only very briefly. If a system has a mirror symmetry, there is a natural decomposition of the Hamiltonian into even and odd parts which makes it possible to consider one-half of the structure with the Neuman or Dirichlet condition, respectively, at the symmetry axis. Next there is the Dirichlet-Neumann bracketing which in combination with the minimax principle says that the jth eigenvalue below the bottom of the continuum can be estimated from above (below) by the jth eigenvalue of the same operator with an additional Dirichlet (Neumann) condition. This is useful if we are able to place an additional condition in such a way that the obtained system is solvable. Recall the observation of Avishai *et al.*[10] that a sharply broken tube can accommodate in the bend a rectangular box wider than the tube itself and long enough; from here it follows that the number of bound states in such a channel is large for bending angles close to $180°$.

In our present case the problem has two mirror symmetries with respect to the axis of the angle θ which we call the scissor axis and with respect to the axis of the larger angle $180°$-θ which we call the second axis. These symmetries

allow us to study thus one-half (to which the trick of Ref. 10 can be applied) or even one-quarter of the scissor. In the latter case the angle dependence of eigenvalues can be studied by perturbation theory using a scaling transformation of the longitudinal variable.[19] The described considerations yield the following conclusions.

(i) Every bound state is even with respect to the scissor axis.

(ii) With respect to the second axis the bound states can have either parity which is alternating if the bound states are arranged according to their energies.

(iii) As θ becomes smaller new bound states emerge from the continuum. The number N of bound states satisfies the inequality $N \geqslant 2c\pi^{-1}(90°/\theta)$ with $c=(1-2^{-2/3})^{3/2} \approx 0.225$. While it is not good around $\theta=90°$, where we know that $N=1$ from Ref. 7, it is asymptotically exact as $\theta \to 0$,

(iv) All the bound-state energies are monotonously increasing functions of θ.

The angle dependence of the bound-state energies has different regimes. In the weak-coupling regime when the scissors are closing and just passed the critical angle θ_c at which a new bound state appeared, our numerical analysis shows that the binding energy of the weakly coupled states behaves as $\approx \pi^2 - \gamma(\theta_c - \theta)^2$ with some constant γ which depends on the particular state. On the other hand, strongly bound states corresponding to a small θ are in the leading order determined by the one-dimensional potential well given by the lowest transverse eigenvalue.[20] The second axis determining the parity of the solution is then deep in the classically forbidden region, so we can conclude that the following.

(v) As θ becomes smaller the bound states group into pairs with opposite parities and the energy gap between them is exponentially small as $\theta \to 0$.

After these general results let us pass to the numerical solution. We use three different methods. The most common among them is the boundary integral method.[21] In combination with the above general results, it provides rather complete information about the discrete spectrum.

On the other hand, the boundary integral method tells us nothing about the scattering problem in the scissor structure. We are interested in particular in the scattering resonances associated with quasibound states, which are characterized by complex values of energy at which the analytically continued resolvent has a pole singularity. A suitable method to treat this problem is the exterior complex scaling. The method was suggested in the seminal paper in Ref. 22 and has developed into an efficient computational tool—see Ref. 23 and references therein. The use of exterior complex scaling for waveguide structures was first proposed in Ref. 24; here we employ it in the form presented in Ref. 25. Before the proper scaling we pass to right-angle scissors by means of the coordinate change

$$x' = x \sin\theta - y\cos\theta,$$

$$y' = y, \tag{1}$$

which takes the Hamiltonian to a unitarily equivalent operator acting as

$$\hat{H}\Psi = \left(-\frac{\partial^2}{\partial x'^2} - \frac{\partial^2}{\partial y'^2} + 2\cos\theta \frac{\partial^2}{\partial x' \partial y'} \right)\Psi. \tag{2}$$

Now we apply the scaling transformation to the longitudinal variable in the structure arms which leaves the central area unchanged, $x=g(X)$ and $y=g(Y)$, which yields the scaled Hamiltonian

$$\hat{H} = -\nabla\left[\begin{pmatrix} c_{11}(X,Y) & c_{12}(X,Y) \\ c_{21}(X,Y) & c_{22}(X,Y) \end{pmatrix} \nabla \right] + U(X,Y), \tag{3}$$

with

$$c_{11}(X,Y) = \frac{1}{g'^2(X)}, \quad c_{12}(X,Y) = -\frac{\cos\theta}{g'(X)g'(Y)},$$

$$c_{21}(X,Y) = -\frac{\cos\theta}{g'(X)g'(Y)}, \quad c_{12}(X,Y) = \frac{1}{g'^2(Y)},$$

and

$$U(X,Y) = \frac{2g'(X)g'''(X) - 5g''^2(X)}{4g'(X)^4} + \frac{2g'(Y)g'''(Y) - 5g''^2(Y)}{4g'(Y)^4} + \frac{g''(X)g''(Y)}{4g'^2(X)g'^2(Y)} 2\cos\theta.$$

The function $g(x)$ can be chosen, e.g., as

$$g(x) = \begin{cases} x & \text{if} \quad |x| \leqslant x_0, \\ \alpha f(x) & \text{if} \quad |x| > x_0, \end{cases}$$

with x_0 larger than the channel half-width and the interpolating function $f(x)$ such that $f(x)=x$ for $|x|>2x_0$, the function $g(x)$ is 3 times differentiable, and the inverse map g^{-1} exists. As long as the parameter α is real, the above transformation is a simple coordinate change which does not modify the spectrum. However, if α assumes complex values, we observe a different behavior in the discrete and continuous part typical in such situations[18]: each branch of the continuous spectrum of the operator (3) is rotated into the complex plane, giving

$$\cup_{n=1}^{\infty} \{(n\pi)^2 + \alpha^{-2}\langle 0, \infty)\}$$

for $d=1$. If $\mathrm{Im}\,\alpha > 0$, the rotated branches point to the lower half-plane and reveal parts of other sheets of the Riemann surface of energy and we are able to see the resonance poles as complex eigenvalues of the transformed operator; the corresponding eigenfunctions are after the transformation decaying at large distances, instead of the original growing oscillations typical for Gamow functions.

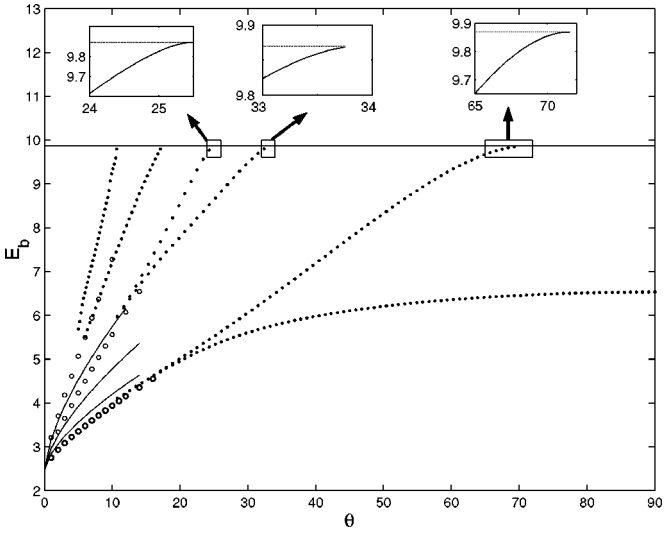

FIG. 1. Bound-state energies for scissors structure as a function of the interior angle θ. The complex scaling method data are shown by points. The boundary integral method data are shown by circles. The asymptotic formulas (5) with corresponding quantum numbers $m=1,2,3$ are given by thin solid lines. Insets above show a blowup of asymptotic behavior of the bound-state energies in the vicinity of bottom of propagation band π^2.

Finally, the third method is based on application of small time-periodic perturbations. The bound states with energies below the propagation subband ($E_b<E_0=\pi^2$) do not participate in stationary transmission. However, it is possible to mix the bound state $|b\rangle$ with propagating state $|k\rangle$ via a time-periodic perturbation

$$V(t)=V_0\cos(\omega t) \tag{4}$$

provided that the matrix elements of the perturbation $\langle b|V|k\rangle\neq 0$. Such a possibility was demonstrated for the for electron transmission in a four-terminal Hall junction influenced by a radiation field.[15,26] Later the mixing of bound states with propagating modes was also realized in a microwave transmission.[16] In analogy with Ref. 27 we use here the time-periodic perturbation (4) as a probing instrument to find the bound-state energy by resonant features in the transmission probability.

III. NUMERICAL RESULTS

Let us show results of the numerical analysis based on the methods described above. First we plot the bound-state energies as functions of the scissor angle θ. The results of complex scale method are presented in Fig. 1 by points.

The results of the boundary integral method are shown in Fig. 1 by circles. For the limit $\theta\to 0$ the energies of bound states are derived in Ref. 13 and have the following form:

$$E_{nm}\approx\frac{\pi^2}{4}\,[n^2+(2n^2+m^2/4)\,\theta^{2/3}+\cdots], \tag{5}$$

where the quantum numbers $n,m=1,2,3,\ldots$, of which, of course, only $n=1$ gives rise to bound states. The factor 1/4 in Eq. (5) takes into account that the width of an inscribed rectangle can approach twice the single channel width for small θ as in the case of broken waveguide studied in Refs. 12 and 13. The upper insets show a blowup of the asymptotic behavior of the energies in the vicinity of the continuum threshold, $E_0=\pi^2$. For all energies of the bound states the asymptotics are $\pi^2-\gamma(\theta_c-\theta)^2$, where γ is a state-dependent constant.

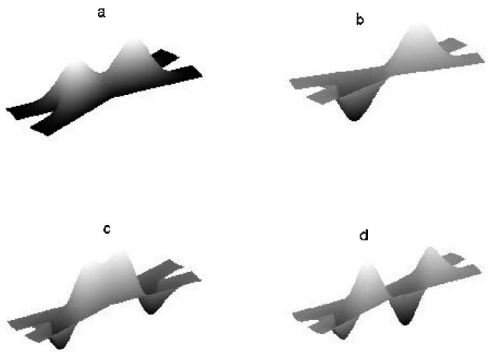

FIG. 2. The first two even-even and odd-even bound states for scissors structure for $\theta=30°$.

It was discussed above that as the angle θ diminishes and the states become strongly bound, the energy gap between the even and odd members of the pair vanishes exponentially fast. Indeed, one can see in Fig. 1 that the second bound-state energy approaches the first one, the fourth bound-state energy approaches the third one, and so on. In Figs. 2(a) and 2(b) the first (even-even) and the second (odd-even) bound states are shown. The eigenfunctions resemble similar quantum mechanical systems with a double-well potential[29] in which an energy distance between the first and second energy levels becomes exponentially small with the growth of the potential barrier between the wells. Figures 2(c) and 2(d) demonstrate the next pair of the bound states in the scissor structure.

With the change of parameters a bound state often transforms into a quasibound state which is manifested as an resonant dip or peak in transmission through the structure—for an example similar to the present one see Ref. 28. As one can see from Fig. 3 the numerically computed transmission through the scissor's structure does not show any resonant features for $\theta>\theta_c\approx 71.5°$. We have also used the time-periodic perturbation method to search for the quasibound states above θ_c. The results of the computation in the vicinity of critical angle θ_c are shown in Fig. 4.

One can see there that for $\theta<\theta_c$ there is a clear resonance effect revealed by mixing the propagating mode with the bound state by the time-periodic perturbation. On the other hand, for $\theta>\theta_c$ these resonant features are vanishing and the transmission probability decays with increasing angle θ. The small wiggle around the value 9.8704 is an artifact of the computation which diminishes with the decrease of V_0.

Moreover, as θ approaches θ_c the transmission probability $T(E)$ slope with respect to the energy E is increasing in the vicinity of E-π^2. In the limit $\theta\to\theta_c$ the derivative dT/dE diverges. If one plots the values E-π^2 at which the transmission reaches one-half (shown by circles in Fig. 3) versus the angle of scissor waveguide, we obtain the remark-

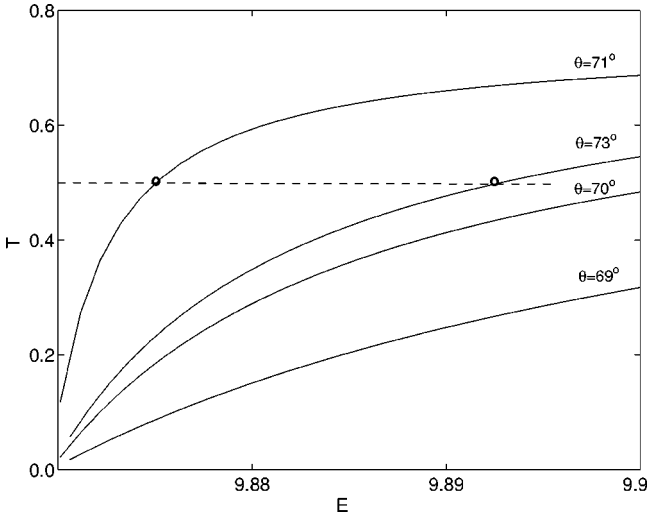

FIG. 3. The probability of transmission through the scissors structure as function of the eigenvalue $E=\lambda k^2$ of the Helmholz equation (16). The probability approaches zero for $E\to E_0=\pi^2$. The circles show for which E the transmission probability equals one-half.

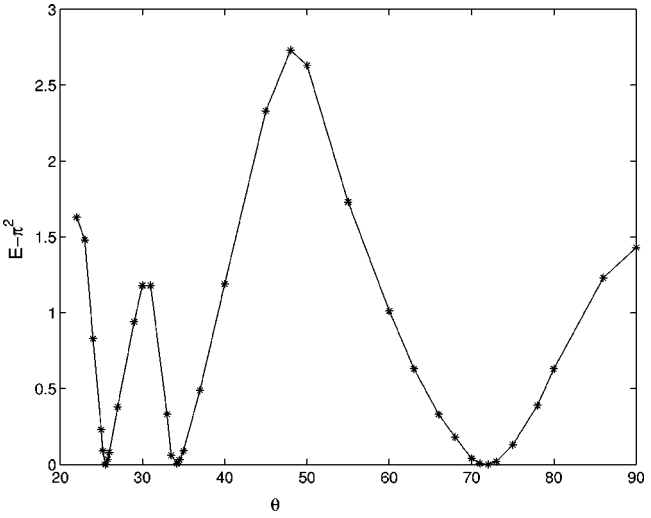

FIG. 5. Distances from the bottom of the propagation band at which the transmission probability takes the value of one-half (see Fig. 3) vs the angle of the scissors.

able curve shown in Fig. 5. We see that this E-π^2 vanishes exactly at the critical angles where new bound states emerge from the continuum.

IV. FERRITE FILLED MICROWAVE WAVEGUIDES AS A WAY TO VARY THE ANGLE OF THE SCISSORS

After analyzing the scissor spectrum, let us discuss how such a structure can be realized experimentally as a microwave device. It is no problem, of course, to build crossed waveguides in the ways explained in Ref. 17. However, in such a setting it is not easy to vary the geometry continuously. Our point here that this goal can be achieved with a structure of a fixed angle if the latter is filled by a ferrite with an axial magnetic anisotropy and an external magnetic field is applied. We will show that this leads to an effective angle controlled by the field strength, following an idea which was first applied to the equivalence between a ferrite-filled squared resonator with an external magnetic field and a field-free rhombic polygon.[30]

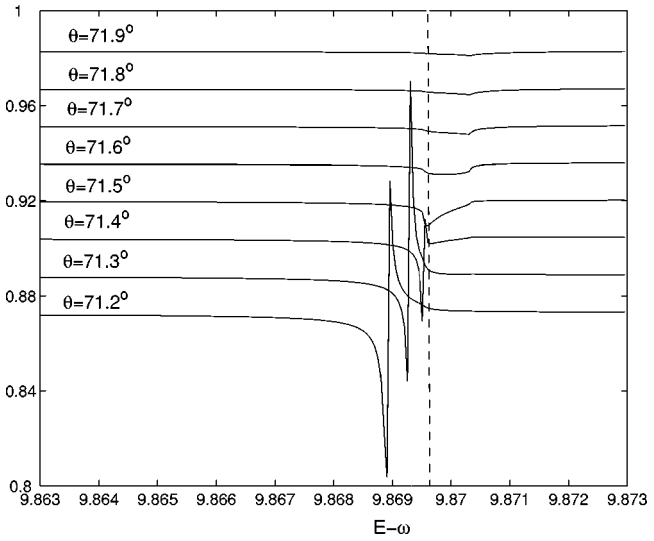

FIG. 4. Evolution of resonant features for the transmission through the scissor structure found by mixing the propagation state with the bound state via the time-periodic perturbation (4) as the angle of the scissor θ increases. The angle dependence is an exact continuation of the bound-state asymptotics shown in the inset of Fig. 1 for $\theta\to\theta_c-0$. For the angles above θ_c resonant features are missing. The dashed vertical line shows the edge of the propagation band, $E_0=\pi^2$.

To explain the mechanism of this equivalence we begin with the Maxwell equations which in the presence of a material have the form

$$\nabla\cdot\mathbf{E}=\nabla\cdot\mathbf{B}=0,$$

$$\nabla\times\mathbf{E}=-ik\mathbf{B},\quad \nabla\times\mathbf{H}=ik\mathbf{E},$$

$$\mathbf{B}=\hat{\mu}\mathbf{H}, \tag{6}$$

where **E** is the electric field, **H** is the magnetic field, **B** is the magnetic induction, $k=\omega/c$, and ω is an eigenfrequency with the wave vector k. We suppose that the material has a magnetic anisotropy corresponding to an anisotropic permeability $\hat{\mu}=1+4\pi\hat{\chi}$ with[31]

$$\hat{\chi}=\begin{pmatrix}\chi_{xx} & \chi_{xy} & 0\\ \chi_{xy} & \chi_{yy} & 0\\ 0 & 0 & 0\end{pmatrix}, \tag{7}$$

where

$$\chi_{xx}=\frac{g\Omega_1 M_0}{\Omega_1\Omega_2-\omega^2},\quad \chi_{yy}=\frac{g\Omega_2 M_0}{\Omega_1\Omega_2-\omega^2}$$

and [Eq. (3)]

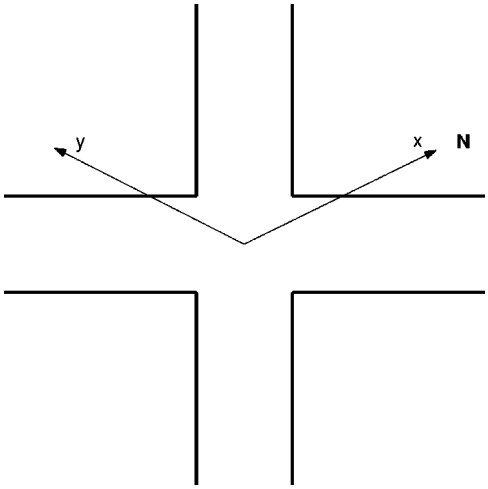

FIG. 6. Schematical view of the cross-bar resonator (scissors with $\theta=90°$) filled with ferrite where **M** is the magnetization of ferrite and **N** is the anisotropy field.

$$\chi_{xy}=-\chi_{yx}=\frac{i\omega g\Omega_1 M_0}{\Omega_1\Omega_2-\omega^2}. \tag{8}$$

Here g is the magnetomechanical factor, M_0 is the magnetization of the material,

$$\Omega_1=gM_0\left(\frac{\mathbf{M}_0\mathbf{H}_0^{(i)}}{M_0^2}+\frac{gK_a}{M_0}\cos^2\Psi\right),$$

$$\Omega_2=gM_0\left(\frac{\mathbf{M}_0\mathbf{H}_0^{(i)}}{M_0^2}+\frac{gK_a}{M_0}\cos 2\Psi\right), \tag{9}$$

and K_a characterizes the anisotropy type: it is an easy-plane anisotropy for $K_a>0$ and an easy-axis anisotropy for $K_a<0$. In what follows we suppose that the material has an easy-plane magnetic anisotropy $K_a>0$, in which case the intrinsic magnetic field is equal to

$$\mathbf{H}=\mathbf{H}_0-4\pi M_{0z}.$$

In the relations (9), Ψ is the angle between the anisotropy axis **N** and the magnetization $\mathbf{M}_0$. We choose the latter to coincide with the z axis along the magnetization, while the x axis lies in the plane spanned by the vectors **N** and $\mathbf{M}_0$.

In the simplest case of an easy plane magnetic material we have $\mathbf{M}_0\perp\mathbf{N}$ and $\mathbf{M}_0\|\mathbf{H}_0^{(i)}$ with $\Psi=\pi/2$, so we obtain from Eqs. (9)

$$\Omega_1=g(H_0-4\pi M_0),$$

$$\Omega_2=g(H_0-4\pi M_0)+gK_aM_0. \tag{10}$$

This is shown in Fig. 6 where the z axis is perpendicular to the plane of the waveguide.

We seek a two-dimensional solution of the Maxwell equations (6) shown at this figure in the form $\mathbf{E}(x,y)=E(x,y)\mathbf{e}_z$. The fields $\mathbf{B},\mathbf{H}$ lay in the plane x,y and depend on x,y too. Then the first equation is satisfied, while the third one gives

$$-ikB_x=\frac{\partial E_z}{\partial y},\quad -ikB_y=-\frac{\partial E_z}{\partial x}, \tag{11}$$

and finally, the fourth Maxwell equation can be rewritten as

$$ikE_z=\frac{\partial H_y}{\partial x}-\frac{\partial H_x}{\partial y}. \tag{12}$$

Using the explicit form of the permeability given by Eq. (7) we get

$$\mathbf{B}=\begin{pmatrix}\mu_{xx} & \mu_{xy} & 0\\ \mu_{yx} & \mu_{yy} & 0\\ 0 & 0 & 1\end{pmatrix}\begin{pmatrix}H_x\\ H_y\\ H_z\end{pmatrix}.$$

Combining this with Eq. (11) we obtain

$$\begin{pmatrix}H_x\\ H_y\end{pmatrix}=\frac{1}{D}\begin{pmatrix}\mu_{yy} & \mu_{xy}\\ \mu_{yx} & \mu_{xx}\end{pmatrix}\begin{pmatrix}\frac{i}{k}\frac{\partial E_z}{\partial y}\\ \frac{-i}{k}\frac{\partial E_z}{\partial x}\end{pmatrix}, \tag{13}$$

where we have denoted

$$D=\mu_{xx}\mu_{yy}-\mu_{xy}\mu_{yx}.$$

Substituting Eq. (13) into Eq. (12) we obtain

$$\mu_{xx}\frac{\partial^2 E_z}{\partial x^2}+\mu_{yy}\frac{\partial^2 E_z}{\partial y^2}+(\mu_{xy}+\mu_{yx})\frac{\partial^2 E_z}{\partial x\partial x}+Dk^2E_z=0. \tag{14}$$

The key observation is that the mixed derivatives in the last equation can be eliminated by the coordinate transformation

$$\begin{pmatrix}x'\\ y'\end{pmatrix}=\begin{pmatrix}-\frac{\sqrt{\mu_{xx}\mu_{yy}-(\mu_{xy}+\mu_{yx})^2/4}}{m u_{xx}} & 0\\ -\frac{\mu_{xy}+\mu_{yx}}{2\mu_{xx}} & 1\end{pmatrix}\begin{pmatrix}x\\ y\end{pmatrix}, \tag{15}$$

which allows us to cast Eq. (14) into the following simple form

$$\nabla^2E_z+\lambda k^2E_z=0, \tag{16}$$

where

$$\lambda=\sqrt{\frac{\mu_{yy}}{\mu_{xx}}}; \tag{17}$$

we have taken into account that $\mu_{xy}+\mu_{yx}=0$ holds in accordance with Eq. (8).

The transformation (15) defines a relation between a right-angle cross structure and a skewed one with an angle defined by λ. It is too daring, however, to speak about a full equivalence, because it is clear from the formulas expressing the elements of Eq. (7) that the angle depends on the eigenfrequencies involved. Let us ask under which conditions this dependence of the geometrical factor (17) can be suppressed. Substituting into Eq. (17) the expressions (10) we get

$$\lambda^2=\frac{\Omega_1\Omega_2-\omega^2+4\pi g\Omega_2 M_0}{\Omega_1\Omega_2-\omega^2+4\pi g\Omega_1 M_0}. \tag{18}$$

Following Ref. 30 we can simplify this expression by assuming that

$$gK_a/M_0 \gg \max\{gH_0, 4\pi g M_0, \omega\}. \tag{19}$$

For typical ferrites $K_a \sim 10^6$ erg/cm^3 and $4\pi M_0 \sim 100$ Oe.[31] Taking the magnetomechanical factor $g \sim 10^7$ sec^{-1} Oe^{-1} we obtain, from Eq. (19), $H_0 \ll 10^4$ Oe and $\omega \ll 10^{11}$, which would require very wide waveguides of width $d \sim 10$ cm. However, there are ferrites with $K_a \sim 10^8$ erg/cm^3 which lead to the inequality $\omega \ll 10^{13}$. Hence in this case we are able to use standard waveguides, the width of which is of order 1 cm. Then we can simplify the geometrical factor of the waveguide to the form

$$\lambda^2=\frac{H_0}{H_0-4\pi M_0}. \tag{20}$$

This formula gives a remarkable possibility to change the angle of the scissors,

$$\theta = 2\arctan\lambda, \tag{21}$$

by means of an external magnetic field applied along the magnetization direction.

Moreover, if to apply a strong magnetic field $gH_0 \gg \omega$ or $H_0 \gg 10^4$ Oe, then it follows from formula (18) that

$$\lambda^2=\frac{H_0}{H_0+gK_a/M_0}. \tag{22}$$

In this case also the effective angle of the structure can be tuned by variation of the external magnetic field.

V. CONCLUSIONS

We have analyzed spectral properties of a scissor structure consisting of two straight waveguides of equal width which cross at an angle θ. The existence of bound states with energies which are increasing functions of the angle θ has been demonstrated both theoretically and numerically. The mechanism responsible for their existence is the same as in similar systems.[7,10,12] The scissor structure has a mirror symmetry with respect to the axis of the complement angle 180°-θ and the bound states exist in pairs differing by parity. We have shown that as the angle θ diminishes the energy gap between the even and odd states of such a pair vanishes exponentially fast. Using the boundary integral method we have also studied the behavior around the critical values θ_c where the bound states emerge from the continuum. Our numerical analysis shows that the binding energy of the weakly coupled states behaves as $\approx \pi^2-\gamma(\theta_c-\theta)^2$ for θ slightly below θ_c. We have also analyzed resonant features in scattering. Furthermore, we have found that in the vicinity of the critical angles the energy derivative of the transmission probability, $dT(E)/dE$, diverges. Finally, we have shown how the angle dependence of the spectrum in such a system can be measured in an electromagnetic setting with right-angle scissors filled by a ferrite material. The effective angular variation can be easily achieved by an external magnetic field applied normally to the plane of the scissor structure.

ACKNOWLEDGMENTS

This work has been partially by RFBR Grant No. 01-02-16077, Grant No. A1048101 of the GAAS (P.E.), and the Royal Swedish Academy of Sciences (A.S.).

*Electronic address: exner@ujf.cas.cz
†Electronic address: almsa@ifm.liu.se

[1] F. Ursell, Proc. R. Soc. London, Ser. A **47**, 79 (1952).
[2] M.L. Roukes, A. Scherer, S.J. Allen, Jr., H.G. Craighead, R.M. Ruthen, E.D. Beebe, and J.P. Harbison, Phys. Rev. Lett. **59**, 3011 (1987).
[3] G. Timp, H.U. Baranger, P. de Vegvar, J.E. Cunningham, R.E. Howard, R. Behringer, and P.M. Mankiewich, Phys. Rev. Lett. **60**, 2081 (1988).
[4] P. Exner and P. Šeba, J. Math. Phys. **30**, 2574 (1989).
[5] P. Exner, P. Šeba, and P. Šťovíček, Czech. J. Phys., Sect. B **B39**, 1181 (1989).
[6] P. Exner, Phys. Lett. A **141**, 213 (1989).
[7] R.L. Schult, D.G. Ravenhall, and H.W. Wyld, Phys. Rev. B **39**, 5476 (1989).
[8] F.M. Peeters, Superlattices Microstruct. **6**, 217 (1989).
[9] P. Exner and P. Šeba, Phys. Lett. A **144**, 347 (1990).
[10] Y. Avishai, D. Bessis, B.G. Giraud, and G. Mantica, Phys. Rev. B **44**, 8028 (1992).
[11] J. Goldstone and R.L. Jaffe, Phys. Rev. B **45**, 14 100 (1992).
[12] J.P. Carini, J.T. Londergan, K. Mullen, and D.P. Murdock, Phys. Rev. B **46**, 15 538 (1992).
[13] J.P. Carini, J.T. Londergan, K. Mullen, and D.P. Murdock, Phys. Rev. B **48**, 4503 (1993).
[14] J.P. Carini, J.T. Londergan, D.P. Murdock, D. Trinkle, and C.S. Yung, Phys. Rev. B **55**, 9842 (1997).
[15] E.N. Bulgakov and A.F. Sadreev, JETP Lett. **66**, 431 (1997).
[16] E.N. Bulgakov and A.F. Sadreev, Tech. Phys. **46**, 1281 (2001).
[17] J.T. Londergan, J.P. Carini, and D.P. Murdock, *Binding and Scattering in Two-Dimensional Systems: Applications to Quantum Wires, Waveguides and Photonic Crystals* (Springer, Berlin, 1999).
[18] M. Reed and B. Simon, *Methods of Modern Mathematical Physics, IV. Analysis of Operators* (Academic Press, New York 1978), Sec. XIII.15.
[19] T. Kato, *Perturbation Theory for Linear Operators*, 2nd ed. (Springer, Berlin 1976), Sec. VIII.6.
[20] F. Bentosela, P. Exner, and V.A. Zagrebnov, Phys. Rev. B **57**, 1382 (1998).
[21] R.J. Riddel, Jr., J. Comput. Phys. **31**, 21 (1979); **31**, 42 (1979).
[22] J. Aguilar and J.-M. Combes, Commun. Math. Phys. **22**, 269 (1971).
[23] N. Moiseyev, Phys. Rep. **302**, 212 (1998).
[24] P. Duclos, P. Exner, and P. Šťovíček, Ann. Inst. Henri Poincaré: Phys. Theor. **62**, 81 (1995).
[25] P. Šeba, I. Rotter, M. Muller, E. Persson, and K. Pichugin, Phys. Rev. E **61**, 66 (2000).

[26] E.N. Bulgakov and A.F. Sadreev, JETP **87**, 1058 (1998).
[27] G. Burmeister and K. Maschke, Phys. Rev. B **59**, 4612 (1999).
[28] P. Exner and D. Krejčiřik, J. Phys. A **32**, 4475 (1999).
[29] L.D. Landau and E.M. Lifshitz, *Quantum Mechanics* (Pergamon Press, New York, 1965).
[30] E.N. Bulgakov and A.F. Sadreev, Europhys. Lett. **57**, 198 (2002).
[31] B. Lax and K.J. Button, *Microwave Ferrites and Ferrimagnetics* (McGraw-Hill, New York, 1962).